



Gasification of pure and mixed feedstock components: Effect on syngas composition and gasification efficiency

Torbjörn A. Lestander^{a,*}, Fredrik Weiland^b, Alejandro Grimm^a, Magnus Rudolfsson^a, Henrik Wiinikka^b

^a Swedish University of Agricultural Sciences, Department of Forest Biomaterials and Technology, SE 901 83, Umeå, Sweden

^b RISE Energy Technology Center, Box 726, SE 941 28, Piteå, Sweden

ARTICLE INFO

Handling Editor: Zhen Leng

Keywords:

Cold gas efficiency
Biomass components
Co-gasification
Wood
Bark
Branches
Needles

ABSTRACT

The aim of this work was to investigate whether the use of individual tree components (i.e., stem wood, bark, branches, and needles of spruces) as feedstocks during oxygen blow gasification is more efficient than using mixtures of these components. Experiments were performed at three oxygen levels in an 18-kW oxygen blown fixed bed gasifier with both single and mixed component feedstocks. The composition of the resulting syngas and the cold gas efficiency based on CO and H₂ (CGE_{fuel}) were used as response variables to evaluate the influence of different feedstocks on gasification performance. Based on the experimental results and data on the composition of ~26000 trees drawn from a national Swedish spruce database, multivariate models were developed to simulate gasifier performance under different operating conditions and with different feedstock compositions. The experimental results revealed that the optimal CGE_{fuel} with respect to the oxygen supply differed markedly between the different spruce tree components. Additionally, the models showed that co-gasification of mixed components yielded a lower CGE_{fuel} than separate gasification of pure components. Optimizing the oxygen supply for the average tree composition reduced the CGE_{fuel} by 1.3–6.2% when compared to optimal gasification of single component feedstocks. Therefore, if single-component feedstocks are available, it may be preferable to gasify them separately because doing so provides a higher gasification efficiency than co-gasification of mixed components.

1. Introduction

High-temperature biomass gasification (Qin et al., 2012a; Weiland et al., 2013; Wiinikka et al., 2017) is a powerful technology for generating a synthetic gas (syngas) rich in H₂ and CO that can be upgraded to motor or aviation fuels via downstream synthesis processes (Sikarwar et al., 2016) such as the production of methanol (Lange, 2001), dimethyl ether, or Fischer-Tropsch fuels (Dry, 2002). An advantage of high-temperature gasification is its low CH₄ yield (Weiland et al., 2015) and the fact that the resulting syngas contains almost no tars (Higman and van der Burgt, 2008). However, biomass-derived soot (Wiinikka et al., 2014, 2018), which is often infused with metallic heteroatoms (Wiinikka et al., 2021), can form from secondary reactions of tar species (Qin et al., 2012b) when gasification is performed above 1000 °C. The process temperature in the reactors of auto-thermal high-temperature gasifiers is mainly controlled by the oxygen to fuel ratio (Weiland et al.,

2015), which also affects the overall gasification efficiency: if the ratio is too high, the chemical energy content of the syngas is reduced because combustion reactions become favored, leading to the formation of H₂O and CO₂ (Weiland et al., 2015). The gasifier's operating conditions must therefore be carefully optimized (see Fig. 1a) to maintain a process temperature high enough to minimize soot formation without sacrificing too much overall gasification efficiency (Wiinikka et al., 2015). Furthermore, it is also important to ask whether gasification of pure feedstocks is more efficient than mixes of those.

Gasification efficiency is normally expressed in terms of the cold gas efficiency (CGE) (Higman and van der Burgt, 2008). Different CGE values can be calculated depending on the intended downstream application of the syngas. For example, if the syngas is to be burned in a gas turbine for power generation, the CGE can be calculated based on the energy stored in all combustible components of the syngas. Conversely, if the syngas is intended for the production of motor fuels or chemicals, the only energetic gas species that can be used in the

* Corresponding author.

E-mail addresses: torbjorn.lestander@slu.se (T.A. Lestander), fredrik.weiland@ri.se (F. Weiland), alejandro.grimm@slu.se (A. Grimm), magnus.rudolfsson@slu.se (M. Rudolfsson), henrik.wiinikka@ri.se (H. Wiinikka).

<https://doi.org/10.1016/j.jclepro.2022.133330>

Received 10 February 2022; Received in revised form 9 June 2022; Accepted 24 July 2022

Available online 31 July 2022

0959-6526/© 2022 The Authors. Published by Elsevier Ltd. This is an open access article under the CC BY license (<http://creativecommons.org/licenses/by/4.0/>).

Nomenclature			
A	number of model components	Nd	needles
\mathbf{b}	vector of coefficients calculated in PLS regression	O ₂	kg oxygen supplied per kg daf biomass
b_i, b_k	(scalar) value of factor i and k , respectively	PCA	principal component analysis
Bk	bark	PLS	partial least squares
Br	branches	Q^2	coefficient of multiple determination (variation predicted by the model)
c	constant	\mathbf{R}	matrix of atomic constituents
CGE	cold gas efficiency all gases in the syngas	R^2	coefficient of variation (variation explained by the model)
CGE_{fuel}	cold gas efficiency based only on CO and H ₂	\mathbf{s}	vector of differences of explained variation between consecutive components
Cs	solid carbon	Sw	stem wood
daf	dry and ash free	\mathbf{T}	transposed vector or matrix
\mathbf{F}	matrix of factors	VIP	important parameter in PLS modelling
\mathbf{f}_c	vector of calibration set residuals	\mathbf{w}_k	vector of weights in the orthogonal PLS algorithm at k components
\mathbf{f}_t	vector of test set residuals using cross validation	\mathbf{X}	matrix of constants, factor values, their squared values, and 2-factor interactions
I	number of observations (rows) in the calibration set	\mathbf{Y}	matrix of response variables
J	number of observations in the test set	y	a single response value (scalar)
K	number of total variables in \mathbf{X} matrix	\mathbf{y}	vector of response values, in our case CGE_{fuel}
λ	lambda; the oxygen to biomass ratio	$\mathbf{y}_p^T \mathbf{y}_p$	sum of squares for the predicted response values
Mx	an equal mixture of all four pure components (Sw, Bk, Br and Nd)	$\mathbf{y}^T \mathbf{y}$	total sum of squares in response
NCV	net calorific value		

downstream synthesis process are CO and H₂. Therefore, only these two gases should be considered in the CGE calculations. The latter gasification efficiency is henceforth referred to as the CGE_{fuel} .

The lignocellulosic biomass of the Northern hemisphere's boreal forests is a major potential resource for biobased syngas production. These forests are the world's largest terrestrial biome and are dominated by conifers such as spruces, as shown in Fig. 1b (U'Ren et al., 2019). In managed forests, young trees are harvested in so-called thinnings

whereas mature trees are mainly cropped in clearcuttings. Biometric studies have been conducted to estimate the growth and yield per unit land area of many tree species, especially those used for timber and pulpwood production. Recently, interest in harvesting whole trees has prompted the development of biomass functions for various above-ground tree components including stem wood, branches, bark, and foliage (Marklund, 1988; Repola, 2008, 2009) as well as stumps and other underground biomass (Pettersson and Stahl, 2006) such as roots.

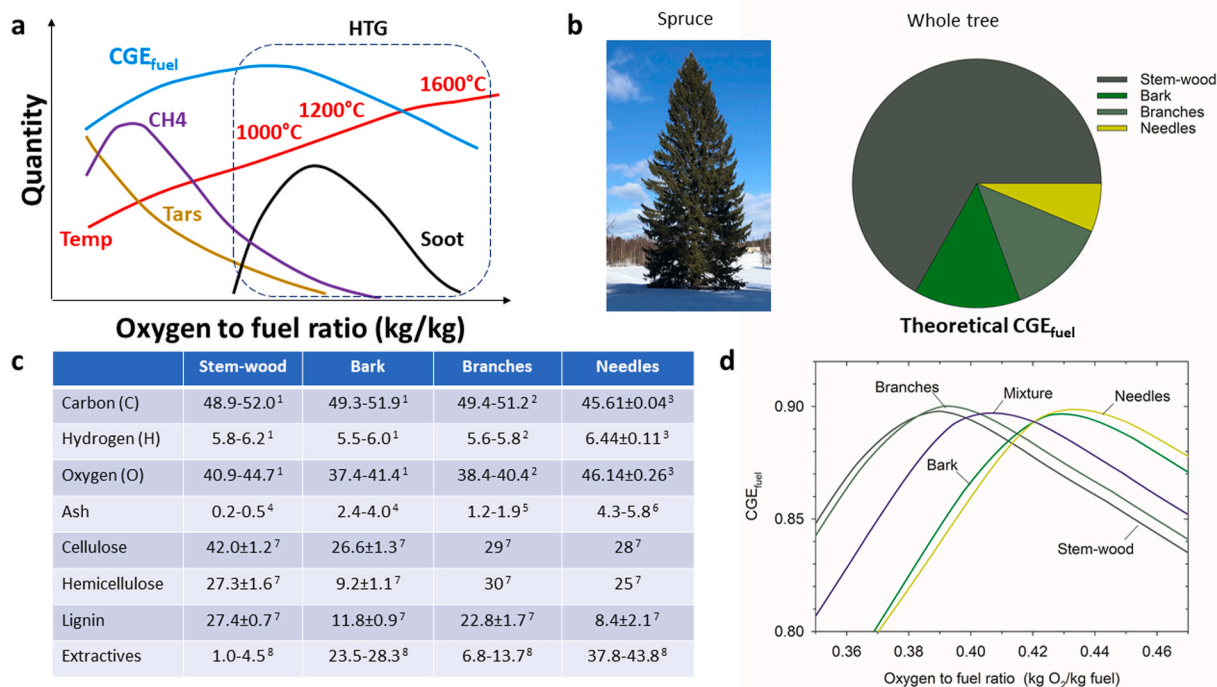


Fig. 1. Fractionated tree gasification. (a) Schematics of important parameters during gasification. (b) Image of a Norway spruce tree and approximate fractions of stem wood, bark, branches, and needles in spruce trees. (c) Chemical composition of four major tree fractions of Norway spruce*. (d) Theoretical gasification efficiency (CGE_{fuel}) for the different tree fractions as a function of oxygen to fuel ratio (kg/kg) based on thermodynamic equilibrium calculations (HTG: high-temperature gasification; CGE_{fuel} : cold gas efficiency fuel). * ¹ Tao et al. (2012); ² Gilbe et al. (2008); ³ Oginni and Singh, 2021; ⁴ Lestander et al. (2012b); ⁵ Wang et al., 2014; ⁶ Werkelin et al. (2005); ⁷ Raisanen and Athanassiadis, 2013; ⁸ Routa et al. (2017).

Feedstock streams derived from logging residues and industrial by-products in the forest-based value chain, here exemplified by Norway spruce, include: (i) pure wood in the form of sawdust, shavings, and chips from sawmills, planing mills, and similar facilities; (ii) branches and tops collected at logging sites (fresh with needles or stored after their shedding) (Nilsson et al., 2015); (iii) bark from the debarking of logs or pulp wood at industrial sites; and (iv) needles collected after shedding (Nilsson et al., 2015) or during logging (Filipsson and Nordén, 2001). These fractions (i.e. wood, bark, branches, and needles) could potentially be used as separate feedstocks for gasification. The masses of each of these fractions in an entire Norway spruce tree relative to the mass of the tree itself are shown in Fig. 1b. The fractions all have distinct chemical compositions (see Fig. 1c) and therefore have different theoretical optimal gasification efficiencies (CGE_{fuel}), which can be estimated by performing thermodynamic equilibrium calculations (see Fig. 1d). It may therefore be beneficial to gasify each fraction separately, since the optimum oxygen-to-fuel ratio for one fraction will not necessarily be optimal for another. For example, the theoretical oxygen-to-fuel ratios needed to achieve the optimal CGE_{fuel} for stem wood and needles (both as received) were ~ 0.39 kg O_2 /kg and ~ 0.43 kg O_2 /kg, respectively. The theoretically optimal oxygen feed rate for gasification of a feedstock mixture containing equal quantities of all four tree components is ~ 0.41 kg O_2 /kg. However, if the feed rate is set to this value but the fuel mixture is inhomogeneous (for example, if the proportions of stem wood and needles entering the gasifier varies over time), the efficiency of the gasification process will oscillate around its theoretical optimum. Specifically, when the share of stem wood is high, the oxygen-to-fuel ratio will be above the optimum value for the fuel mix (supraoptimal), leading to enhanced combustion and high yields of CO_2 and H_2O . Conversely, the oxygen-to-fuel ratio will be below the optimal value (suboptimal) during periods with an increased share of needles in the fuel mix, resulting in high yields of CH_4 and other products of incomplete gasification. This is important because the content of needles in logging residues (branches and tops) varies between 7.5% and 38.7% depending on the extraction conditions (Nilsson et al., 2015). Previous studies have shown that the gas-phase conversion of CH_4 is kinetically limited at typical biomass gasification temperatures (Dupont et al., 2007; Dufor et al., 2009; Jand et al., 2009). Therefore, the gas mixture in the gasifier may not reach thermodynamic equilibrium, in which case the syngas exiting the gasifier will contain elevated levels of CH_4 , as well as CO_2 and H_2O . If this happens, the maximum gasification efficiency based on the yields of CO and H_2 (CGE_{fuel}) will be lower than the theoretical results presented in Fig. 1d.

The aim of this work was therefore to experimentally compare fractionated gasification of separated feedstock components (exemplified by different tree components) to co-gasification of diverse feedstocks. Only a few previous studies have investigated how variation in the chemical composition of forest-based feedstocks influences thermochemical biomass conversion. Werkelin et al. investigated differences in the inorganic composition of different tree parts (Werkelin et al., 2005, 2010) and their influence on ash-related operational problems during combustion (Werkelin et al., 2011). Another study showed that the yield and quality of fast pyrolysis bio-oils depended on the choice of pyrolysis feedstock and which part of the feedstock was used (Oasmaa et al., 2016 and references therein). The effects of wood composition (i.e., the relative contents of bark, branches, and needles) and supercritical CO_2 extraction on charcoal production have also been investigated (Surup et al., 2020), and it was shown that the microstructure of soot formed during high temperature (1100 °C) pyrolysis depends on which tree parts (i.e., needles or branches) are used as the feedstock (Trubitskaya et al., 2021). Other examples of co-gasifying are wood and algae (Zhu et al., 2016), wood and coconut (Sulaiman et al., 2018) and coconut and oil palm (Inayat et al., 2019). However, no previous studies have examined autothermal high-temperature gasification of different tree fractions, the possible benefits of fractional tree gasification, and the possibility of energy losses during co-gasification. This work

therefore focuses on gasification of stem wood, bark, branches, and needles, using Norway spruce as a biomass source and model feedstock. Experiments were performed in a fixed bed oxygen blown gasifier whose gasification performance was previously shown to closely match that achieved in oxygen blown entrained flow gasification (Wiinikka et al., 2017).

2. Materials and methods

2.1. Biomass model

Gymnosperms, especially spruces, dominate the boreal forest of the northern hemisphere, so Norway spruce (*Picea abies* Karst. (L.)) was chosen as a model species capable of providing large quantities of lignocellulosic biomass. A selection of trees was cut at the stem base and branches were cut near the surface of the stem. The stems were then debarked. Each branch was divided into twigs (i.e., green needles and fine terminal shoots <5 mm in diameter), and other parts (i.e., coarser parts of the branch consisting of wood and bark), which were collected separately. Four tree components were thus collected: stem wood, branches, bark, and needles (including fine shoots), representing the main commercial forest-based feedstocks. Additional fresh Norway spruce bark was collected from the SCA Timber sawmill at Rundvik, Sweden. The materials were chipped, dried to about 10% moisture content, and then ground with a 4 mm sieve before pelletizing. A fuel mixture containing equal quantities of each of the four abovementioned fuel assortments (i.e. 25 wt% each of stem wood, bark, branches and needles) was also prepared.

2.2. Pelletizer

The collected biomass types were pelletized using a PP 150 pelletizer (Sweden Power Chippers) at the Biomass Technology Centre within the Swedish University of Agricultural Sciences in Umeå, Sweden. The press channel diameter and length were 8 and 55 mm, respectively.

2.3. Gasifier

Gasification experiments were performed in a pilot gasifier at the RISE Energy Technology Center in Piteå, Sweden. The gasifier and its operating procedure were previously described by Wiinikka et al. (2017). Briefly, the pilot plant features a feeding system, a ceramic-lined reactor, a gas cooler, a gas analysis system, and a furnace for final combustion of the resulting syngas. A schematic depiction of the gasification plant is provided in Fig. 2.

Each pelletized fuel assortment was fed into the gasifier using a mechanical feeding system at a rate of 3.5 ± 0.2 kg dry weight h^{-1} . The pellets were fed from the top of the gasifier and fell to the bed under the influence of gravity. Pure oxygen was used as the oxidant and was supplied to the reactor through three different inlets, each of which was individually controlled by a mass flow controller. The process temperature was controlled by adjusting the proportions of feedstock and oxygen added to the reactor. Slipstreams of the syngas were sampled for analysis as described below. The remaining syngas was combusted in a furnace equipped with an oil burner as a continuous ignition source.

2.4. Fuels and operating conditions

Gasification experiments were conducted on a single experimental day for each of the five fuel assortments. Before each experimental day, the gasifier was heated to approximately 1200 °C overnight using an electric silicon carbide heater (8 kW).

During the gasification experiments, the fuel feeding rate was kept relatively constant, aiming for a thermal load of approximately 18–20 kW. Each fuel was gasified under three different operating conditions according to the experimental design shown in Fig. 3, meaning that the

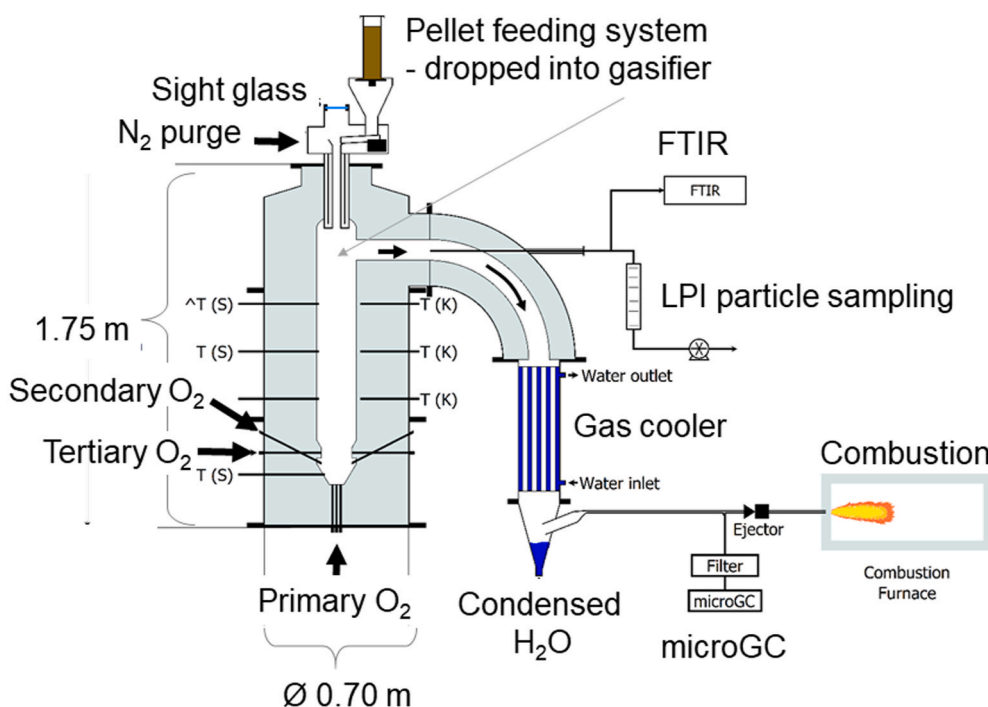


Fig. 2. Schematic picture of the fixed-bed oxygen blown pilot gasifier (FOXBG).

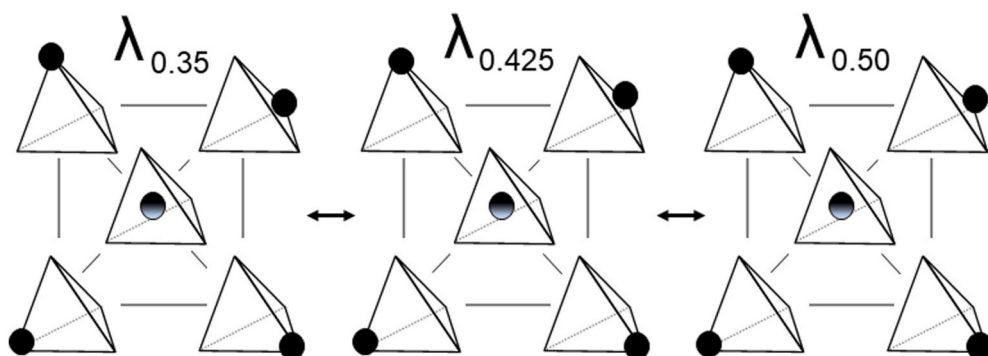


Fig. 3. Experimental design showing pyramids that represent the four materials used (stem wood, branches, bark and needles) in each separate corner (black dot) and a mix of all in the centre of the pyramid for settings of three different levels of oxygen stoichiometric ratio (λ : 0.35, 0.425 and 0.50) in the gasification.

flow rate of oxygen was varied to examine a wide range of practically relevant gasification stoichiometries. The oxygen stoichiometric ratio, λ , is defined as the mass ratio of the supplied oxygen to the oxygen required for stoichiometric combustion (Eq. (1)).

$$\lambda = \frac{O_{2, \text{ supplied}}}{(O_{2, \text{ stoichiometric required}})^{-1}} \quad (1)$$

The gasifier was operated at λ set points of 0.35, 0.425, and 0.50 for each fuel assortment. At each set point, the gasifier was allowed to operate undisturbed for at least 80 min before sampling the syngas to ensure that the char bed was thermally equilibrated and that its composition was representative of the fuel assortment under investigation. In between set points, the fuel feed was stopped to burn off residual char from the bed to avoid influencing the results obtained at the next operating set point. Residual ash was manually removed from the bed to prevent ash buildup in the burner from influencing the gasification experiments.

2.5. Analytical procedures

2.5.1. Fuel characterization

Ultimate and proximate analysis (Table 1) of four separate

Table 1

Proximate and ultimate analysis of tree components (all values given on a dry matter basis).

Analysis	Stem wood (Sw)	Branches (Br)	Bark ^a (Bk)	Needles (Nd)
GCV (kJ/g)**	20.33	20.73	20.33	21.20
NCV (kJ/g)**	18.96	19.38	19.00	19.81
C (wt.%)	50.8	51.7	51.8	51.6
H (wt.%)	6.3	6.2	6.1	6.4
O (wt.%)	42.0	40.5	38.5	36.8
N (wt.%)	<0.1	0.2	0.3	1.0
S (wt.%)	<0.01	<0.01	0.03	0.07
Cl (wt.%)	<0.01	<0.01	<0.01	0.03
Ash (wt.%)	0.8	1.4	3.3	4.1
Volatiles (wt. %)	83.2	80.2	74.8	75.4

^a Rundvik; ** GCV: gross calorific value; NCV: net calorific value.

assortments from spruce trees were performed by two accredited laboratories: Bränslelaboratoriet, Umeå, Sweden and Eurofins Environment Testing Sweden AB, Lidköping, Sweden. The gross calorific value (EN ISO 18125:17), ash content (EN 15403:2011), volatile matter content (EN 15148), and contents of carbon (C), hydrogen (H), nitrogen (N), sulphur (S) (EN ISO 16948:2015), oxygen (O) (EN ISO 18125:17), and chlorine (Cl) (EN ISO 16994:2016) were determined. The concentrations and composition of ash forming elements were also analyzed (data not shown). The composition of the mixed fuel (Mx) was calculated based on the weight fraction and composition of its constituent materials (25% each).

The moisture content and ash mass fraction of the pellets were analyzed in accordance with ISO 18134-2:2015 and 18122:2015, respectively. The pellets' bulk densities were determined according to the ISO 17828:2015 standard and their mechanical durability was measured according to ISO 17831-1:2015. In addition to the variation in chemical composition between the tree components, their pellets varied in terms of their moisture content (which ranged from 7.7 to 9.2%), bulk density (551–698 kg/m³), and mechanical durability (91.4–97.5%). This variation in pellet quality is unlikely to have affected gasification performance given the low feeding rates and the operating conditions that were applied.

2.5.2. Gas analysis

Syngas was sampled from a sampling position upstream of the syngas cooler via a heated line to an FTIR spectrometer (MKS Multigas 2030; MKS Instruments Inc., USA) during periods when particle sampling at this position was not being performed (see Fig. 2). The FTIR spectrometer was used to analyze the concentrations of NH₃, HCN, and H₂O in the syngas. Cooled syngas from a point downstream of the syngas cooler was also sampled using a micro-GC (Varian 490, Agilent Technologies Inc., USA) for analysis of He, H₂, O₂, N₂, CH₄, CO, CO₂, C₂H₂, and C₂H₄. He was used as an internal standard to estimate the syngas yield. Particulate ash matter in the syngas was also sampled but no particle sampling data are presented or analyzed here.

The cold gas efficiency (CGE_{fuel}) for down-stream production (e.g. of liquid fuels) is a measure of gasification efficiency that was used as the overall response variable in the analyses. CGE_{fuel} was calculated for each run as the output net calorific values for CO (283.2 kJ/mol) and H₂ (243.9 kJ/mol) in the syngas relative to the feedstock's net calorific value. This dimensionless variable was used as a discriminator during multivariate modelling and simulation.

2.6. Modelling and diagnostics

Thermodynamic equilibrium calculations were performed using the FactSage database (Bale et al., 2009, 2016) to estimate theoretical adiabatic gasification efficiencies (CGE_{fuel}) for the different pure and mixed tree fractions as functions of the oxygen to fuel ratio (see Fig. 1d). One of the main assumptions in this software is that equilibrium is reached by minimizing Gibbs free energy. In addition, other assumptions are about the same as those given by Habibollahzade et al. (2021) who simulated biomass gasification using various gasification agents.

To obtain an overview of the gathered data, we used principal component analysis (PCA) (Jolliffe, 1986) to generate biplots showing the score and loading values for interesting principal components within the model space – typically the two components explaining the largest proportion of the observed variation. Using matrix notation, the PCA model has the following form:

$$C = [F R Y] = TP^T + E \quad (2)$$

Here, C is a matrix of all collected observations with runs in rows and variables in columns, where the variables are the matrices of experimental factors F, main atomic constituents (C, H, O) in each feedstock R, and responses Y. T is a matrix of vectors with score values, P^T is a

transposed matrix with vectors of loadings, and E contains the residuals. The PCA was performed using the SIMCA software package (Umetrics, Sweden).

The experimental data for each run were modelled as follows:

$$y = a + b_i + b_i \times b_k \quad (3)$$

Here, y is response value, a is a constant, b_i is the observed values of experimental factor i (i = 1, 2, 3 ... n) and b_k is the observed values of factor k (k = 1, 2, 3 ... n). The b_i × b_k term thus corresponds to 2-factor interactions when i ≠ k and squared factor values when i = k. The factors were O₂ (the oxygen supply in kg per kg of dry ash-free biomass, see Nomenclature), the observed gasification temperature, and the proportions of the different feedstocks (Sw, Bk, Br, Nd and Mx) in the gasifier.

The CGE_{fuel} responses for all of the runs were then stored in the vector y. The corresponding constants, factor values, squared factor values, and 2-factor interaction values were stored in the matrix X. The lignocellulosic components of the feedstock were treated as dependent variables because they have many common structural characteristics at the molecular level. For example, lignins contain coniferyl, sinapyl and paracoumaryl units, while cellulose contains glucose. Furthermore, branches contain both wood and bark. Because the gathered data featured dependencies in both rows and columns, partial least squares (PLS) regression techniques (Wold et al., 1983) were used to model the CGE_{fuel} response. The PLS regression model can be expressed as follows using matrix notation:

$$y = Xb + f \quad (4)$$

Here, b is the vector of PLS regression coefficients and the residuals are collected in f.

The metrics used to evaluate the PLS models were the variance explained (R²) and predicted (Q²) by the model and the variable importance in the projection (VIP):

$$R^2 = 1 - f_c^T f_c (y_c^T y_c)^{-1} \quad (5)$$

$$Q^2 = 1 - f_t^T f_t (y_t^T y_t)^{-1} \quad (6)$$

$$VIP = \{[w^2 s^T][y_p^T A y_p A (y^T y)^{-1} K^{-1}]^{-1}\}^{0.5} \quad (7)$$

3. Results and discussion

3.1. Overview – variation in tree components

Data on sample trees included in the Swedish National Forest Survey during the years 2012–2016 were used to calculate the mass fractions of tree components from Norway spruce trees. A total of 26,833 Norway spruce trees from sample plots all over the Swedish boreal forest were represented in the sample set. Biomass functions (Marklund, 1988) for the different tree components (i.e., stem wood, branches, bark, and needles) were used to perform these calculations; for details, see the Supplementary Information. This made it possible to calculate component fractions (i.e., the relative abundances of stem wood, bark, branches, and needles) for individual assortments (i.e. whole stems, green branches, green branches and tops, and whole trees), as shown in Table 2.

3.2. Overview – parameters and variables in experiment

As mentioned previously, the gasifier was operated at λ values of 0.35, 0.425, and 0.50 for each fuel assortment. Since the stoichiometric oxygen demand differed between the fractions, the amount of oxygen supplied per kg of fuel depended on the chosen feedstock. For details of the gasifier's operating conditions including the C, H, and O mass balances during the experiments, see the Supplementary material.

Table 2

Average, maximum, and minimum tree component fractions for four biomass types (C1–C4) from Norway spruce trees (>7 m in height; std denotes standard deviation).

Assortment	C1 Whole stems		C2 Green branches		C3 Green branches & tops		C4 Whole trees			
	wood	bark	needles	branches	needles	branches ^a	wood	bark	branches ^a	needles
Mean	0.900	0.100	0.366	0.641	0.321	0.679	0.581	0.062	0.224	0.133
Std	0.023	0.023	0.037	0.037	0.057	0.057	0.105	0.004	0.057	0.048
Max	0.954	0.225	0.462	0.735	0.374	0.853	0.858	0.076	0.587	0.340
Min	0.775	0.046	0.265	0.538	0.147	0.626	0.135	0.037	0.070	0.030

^a Including tops for C3 and C4; wood refers to stem wood.

The process temperature during the experiments varied between 1040 and 1200 °C, which is a normal range of reactor temperatures for pilot-scale (20–200 kW) oxygen-blown high-temperature gasification of feedstocks like black liquor (Carlsson et al., 2010) and solid biofuels (Carlborg et al., 2018; Ögren et al., 2018; Weiland et al., 2021; Wiinikka et al., 2017). Somewhat higher reactor temperatures (1100–1500 °C) have been reported during oxygen-blown pressurized entrained-flow gasification of stem wood powder (Weiland et al., 2015, 2016) and torrefied wood residues (Weiland et al., 2014) on larger scales (<1 MW_{th}). The elemental mass balances (C, H, and O; see the Supplementary Information) for each run were close to unity (average = 0.969, standard deviation = 0.044), validating the chosen experimental and analytical approach.

Fig. 4 shows a biplot based on the first two principal components from the PCA. These two principal components collectively explained 67.6% of the overall variation in the screening dataset. The main variable contributing to the first principal component (PC1) is the λ value (which reflects the amount of oxygen in the gasifier), while variables contributing to the second principal component (PC2) are the constituents of the syngas and the tree components. As λ increases (i.e., upon moving in the positive direction along PC1), so does the content of fully oxidized gases (CO₂ and H₂O) in the syngas. These syngas components correlated negatively with CH₄, C₂H₂, C₂H₄ and C(s) because the former

were to the right of the origin (0, 0) along PC1 while the latter were to its left. Additionally, the gases were separated into different groups along PC1 and PC2: CO₂ and H₂O form one group, CO and H₂ form another, and CH₄, C₂H₂, C₂H₄ and C(s) form a third. Collectively, these groups occupy the vertices of a triangle spanning the biplot surface. A similar triangular pattern is seen for the N-rich gases NO, NH₃ and HCN (yields, see also Supplementary Information). As expected, the cold gas efficiency calculated based on the H₂ and CO contents of the syngas (CGE_{fuel}) correlated strongly with the contents of CO and H₂ but was negatively correlated with the other gaseous components of the syngas. If the CGE was instead calculated based on all combustible components of the syngas, then CH₄, C₂H₂, and C₂H₄ all contributed to the calculated efficiency, as indicated by the double-headed arrow. Finally, the H (Hp) content of the fuel pellets correlated negatively with their C (Cp) and O (Op) contents.

Within the biplot, the observations for needles (Nd) are clearly separated from those for other tree components. This appears to be related to the high H content of Nd pellets, especially in the case of Nd pellets gasified at the intermediate λ value (Nd2). The datapoints corresponding to the gasification of all five tree components at the lowest λ are located in the lower left quadrant of Fig. 4 in roughly the same place as the syngases CH₄, C₂H₂, and C₂H₄ as well as soot (C(s)). Therefore, as expected, low λ values are associated with higher concentrations of these gasification products.

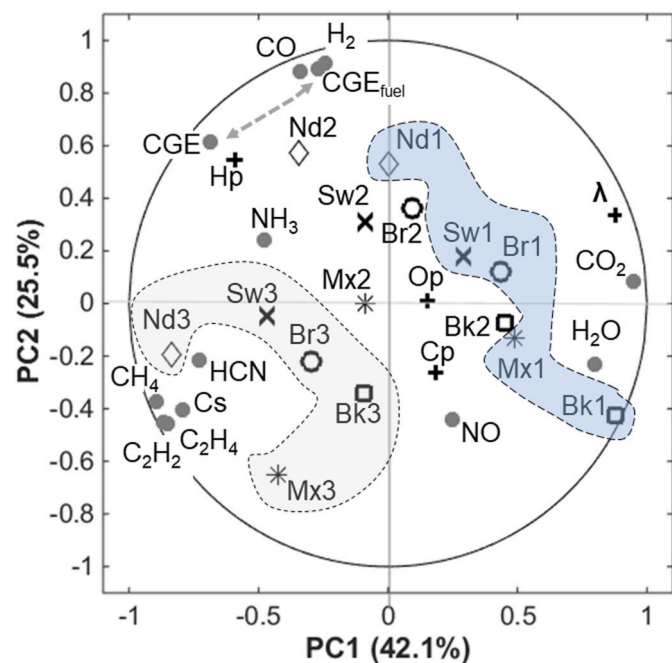


Fig. 4. PCA biplot showing a) parameters (+) i.e. p: pellet concentration of C, H and O and λ : lambda; and b) responses i.e. Sw: x stemwood; Br: o branches; Bk: □ bark; Nd: ◇ needles; Mx: * mix of all; number: 1 (high λ) to 3 (low λ); CO, H₂, CO₂, H₂O, CH₄, C₂H₂, C₂H₄, C₂H₄, NO, NH₃ and HCN are gases; Cs: solid carbon; CGE: cold gas efficiency all gases; CGE_{fuel}: cold gas efficiency CO and H₂. Shaded area up to right is high λ (#1) and the one down to the left is low λ (#3).

3.3. Syngas composition

The yields of major syngas species over λ recalculated to kg O₂ per kg dry ash-free (d.a.f.) biomass for the four different individual spruce fractions and the fuel mixture are shown in Fig. 5. Complete oxygenation of Sw, Br, Bk, Nd and Mx was according to the analysis (Table 1) reached at a supply rate of 1.447, 1.490, 1.536, 1.604 and 1.519 kg O₂ per kg d.a. f. biomass, respectively. The yields of H₂ and CO showed curvature, with a maximum within the tested range of oxygen ratio. This was in accordance with previous experiences using bark residues (Weiland et al., 2021), stem wood (Wiinikka et al., 2017) and predictions when using thermodynamic equilibrium calculations. Increased addition of oxidant to the gasifier resulted in enhanced combustion illustrated by the higher yields of the combustion products H₂O and CO₂. At the same time decomposition of CH₄ (Fig. 5) and other hydrocarbons (not shown here) increased. It was previously shown that the CH₄ yield was also correlated to the gasification temperature, and that a gasification temperature above 1400 °C was required to reach CH₄ concentrations in the syngas below one mol-% (dry, N₂-free syngas) for stem wood biomass (Weiland et al., 2015). Although the measured process temperature never exceeded 1200 °C in this work, the CH₄ concentration was below one mol-% (dry, N₂-free syngas) for the highest oxygen ratios during gasification of bark fuel and fuel mixture, respectively. The actual gasification temperature inside the flame above the fuel bed could of course have been much higher. Due to the curved nature of the CO and H₂ yields described above, the CGE_{fuel} also became curved with maxima within the tested range, Fig. 5.

The yields of CH₄, CO₂ and H₂O were among the highest for the fuel mix (Mx), and almost always higher than for the individual spruce

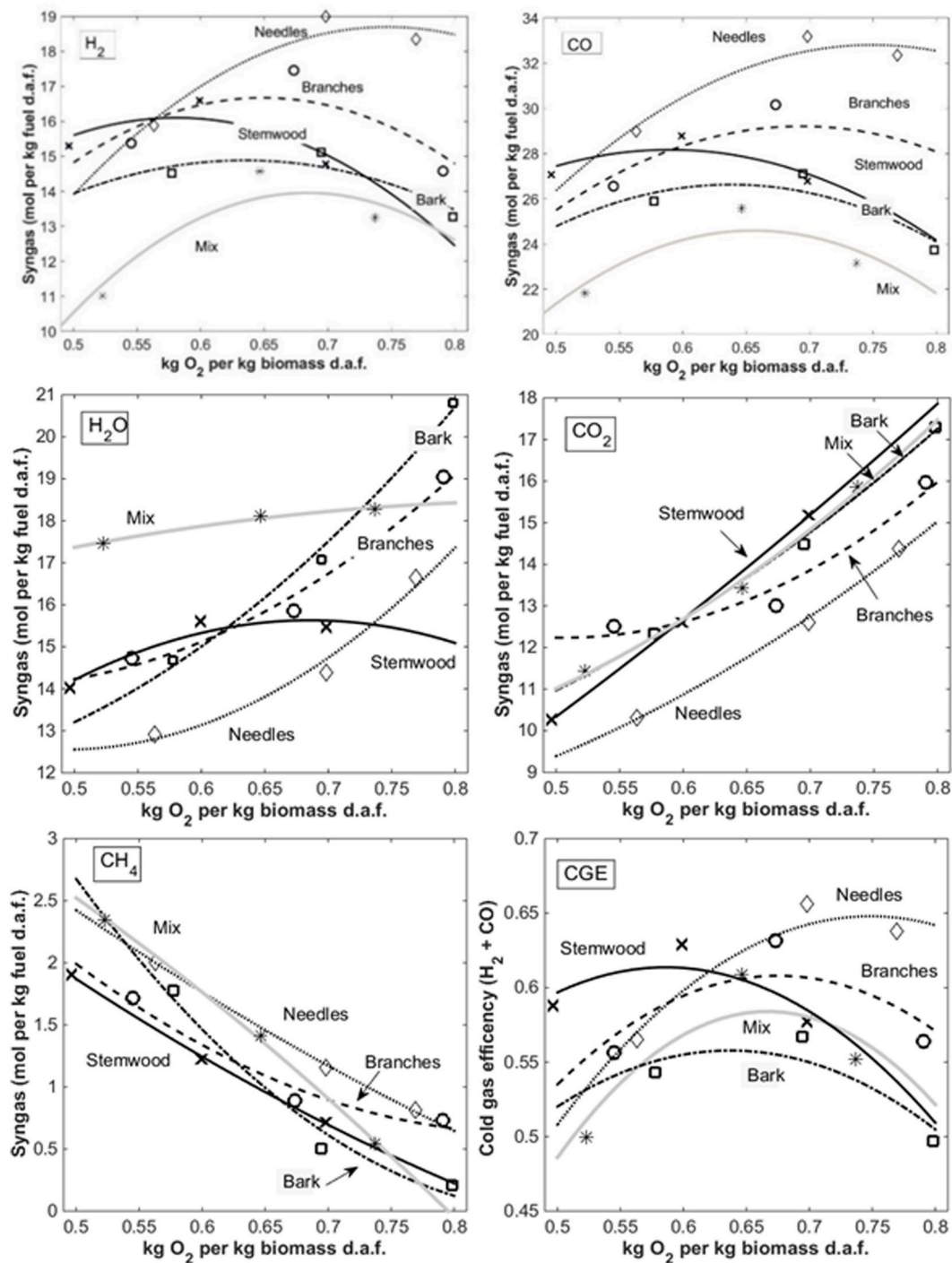


Fig. 5. Yields of H₂, CO, H₂O, CO₂, CH₄ and CGE_{fuel} versus oxygen supply. Lines are 1.5 polynomial fittings (see Supplementary Information) for each tree component (stemwood: x solid black line; bark: □ dash-dot line; branches: o dash line; needles: ◇ dot line; mix; * solid grey line).

fractions at corresponding oxygen-to-fuel ratio (Fig. 5). Consequently, the CGE_{fuel} for the fuel mix was also low compared to the individual spruce fractions, and only slightly higher than the spruce bark at the corresponding oxygen-to-fuel ratio.

3.4. Results of modelling CO and H₂ as CGE_{fuel}

The multivariate CGE_{fuel} model initially included 27 factors: 6 main factors plus the corresponding squared factors and two-way interactions. The correlation between the gasification temperature (an uncontrolled factor) and the oxygen supply was high (0.72), so the model was

simplified by excluding the temperature factor and the associated squared and interaction factors. Several model terms were thus removed without reducing performance. All of the main parameters (O₂, Sw, Bk, Br and Nd) influenced the model to an extent, but Nd and O₂ had the greatest influence. Three of the five remaining squared terms had little influence and were therefore excluded, leaving only the squared terms for O₂ and Sw. Six of the two-way interactions were excluded for the same reason, leaving only the two-way interactions of Nd with Bk, O₂ with Br, and Sw with O₂. In total, only 11 terms pertaining to five PLS components were retained in the final model; Fig. 6 shows their relative influence on the model's output.

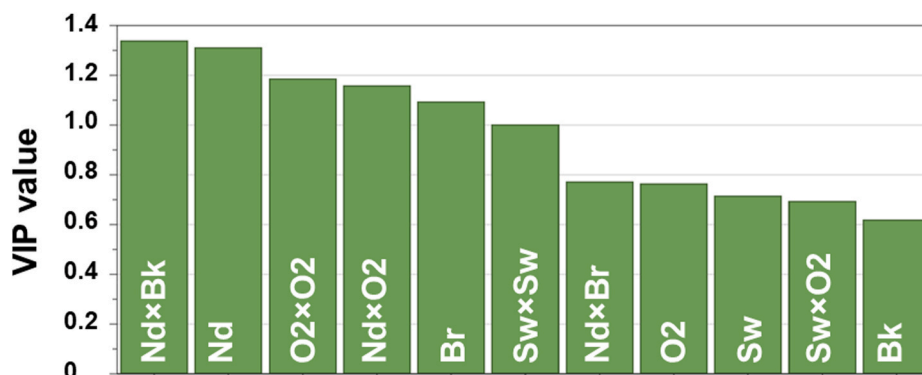


Fig. 6. The VIP value shows variable influence on the PLS projection for the terms in the model (VIP value > 1 indicates above average influence).

The final model with five PLS components was significant ($p < 0.05$) with three degrees of freedom and explained 98.8% (adjusted R_{adj}^2 : 94.2%) of the observed variation in CGE_{fuel} . Its Q^2 value was 0.862, indicating a high predictive ability. Fig. 7 shows the agreement between the CGE_{fuel} values predicted by the model and experiment.

Contour plots showing the variation in the predicted CGE_{fuel} for the gasification of pure and mixed tree component feedstocks under various conditions are presented in Fig. 8. Briefly, each triangular plot shows how CGE_{fuel} varies as the relative abundance of stem wood, needles, and branches in the feedstock is changed. The plots in the top (Fig. 8A-C) and bottom (Fig. 8D-F) rows show the predicted outcomes when the bark content of the feedstock is 3.7% and 7.6%, respectively; these values represent the minimum and maximum observed bark contents of individual spruce trees. The plots in the left, middle, and right columns show predicted outcomes when the oxygen supplied per kg d.a.f. biomass is 0.5, 0.65, and 0.8 kg, respectively. The areas enclosed within dashed lines in each plot correspond to the ranges of the mass fractions of the different components in whole trees (see Table 2).

The contour plots clearly show that the highest CGE_{fuel} values occur at the vertices. This is especially true for the plots in the middle column (Fig. 8B and E), which show the efficiency achieved when the oxygen supply is closest to optimal for each tree component. If the model space was modified such that the bark content of the feedstock was set to 0% or 100%, it would be possible to estimate the optimal oxygen content for each pure feedstock component. The component giving the highest predicted cold gas efficiency based on the CO and H₂ content of the syngas was needles, for which a CGE_{fuel} of 0.749 was obtained. Spruce needles (Nd) contain energy-dense extractives (resins) that are low in oxygen but comparatively rich in hydrogen, which may partly explain their high CGE_{fuel} value in the gasification experiments. The optimal

quantity of oxygen for Nd gasification was 0.704 kg oxygen per kg d.a.f. needle biomass, while the oxygen supply optima (in kg oxygen per kg d. a.f. biomass) and maximum CGE_{fuel} values for Sw, Br, and Bk were 0.585 and 68.6%, 0.669 and 66.0%, and 0.672 and 70.1%, respectively.

As expected, the CGE_{fuel} values predicted by the model were lower than the theoretical maximum efficiencies calculated by assuming thermodynamic equilibrium within the gasifier. It has frequently been argued that this can be attributed to terminal losses and failure to reach thermodynamic equilibrium during experiments. Cold gas efficiencies of 45–85% based on all combustible syngases (including CO, H₂, and all hydrocarbons) were reported in a review by Emami Taba et al. (2012).

The mixed feedstock (Mx) consisted of equal masses of all four tree components. The optimal amount of oxygen for this mixture was predicted to be 0.658 kg, giving a CGE_{fuel} of 60.4%, which is lower than the maximum achievable CGE_{fuel} for any pure component. According to the PLS model, Mx gasification using this optimal oxygen supply would result in CGE_{fuel} losses of 2.9%, 0.2%, 0.2%, and 1.3% when compared to gasification of Sw, Bk, Br, and Nd separately using the optimal oxygen supply for each individual component.

The experimental data made it possible to scan the entire PLS model space to predict the gasification efficiencies for all possible mixtures of the four tree components and their dependence on the oxygen supply. Doing so revealed that if the gasification conditions were optimized for Sw, the CGE_{fuel} for each mass unit of co-gasified Bk, Br and Nd would be 4.3, 4.1, and 8.1 percentage points lower, respectively, than the maximum possible values for these components. Similarly, if the gasification conditions were optimized for Nd, the model predicts efficiency losses of 7.9, 0.7, and 0.7 percentage points for Sw, Bk and Br, respectively.

The stars in the plots presented in Fig. 8 indicate the composition of the average Norway spruce tree; based on the forest inventory data, this average tree contains 58.1% Sw, 6.2% Bk, 22.4% Br, and 13.3% Nd. The optimal oxygen supply for components mixed in these proportions is 0.621 kg per kg d.a.f. biomass. Gasification under these conditions would give CGE_{fuel} values of 66.9%, 66.8%, 64.7% and 68.7% for Sw, Bk, Br and Nd, respectively, corresponding to efficiency losses of 1.3–6.2 percentage points when compared to gasification of the separated components using their individually optimized oxygen supply levels.

Other simulations (see Supplementary Information) were performed assuming the use of commercial assortments such as tree stems or logging residues (see Table 2). For simplicity, each such assortment was assumed to contain only two components. These simulations were based on a more rigid polynomial model as an alternative to the PLS model. For tree stems consisting of 90.0% stem wood and 10.0% bark, the loss in CGE_{fuel} when compared to separate gasification of the two components were small (<0.5 percentage points) and comparable to variation in performance expected as a result of variation in the composition of individual components. This was because the optimal oxygen supply values for stem wood and bark are quite similar. Consequently, using the

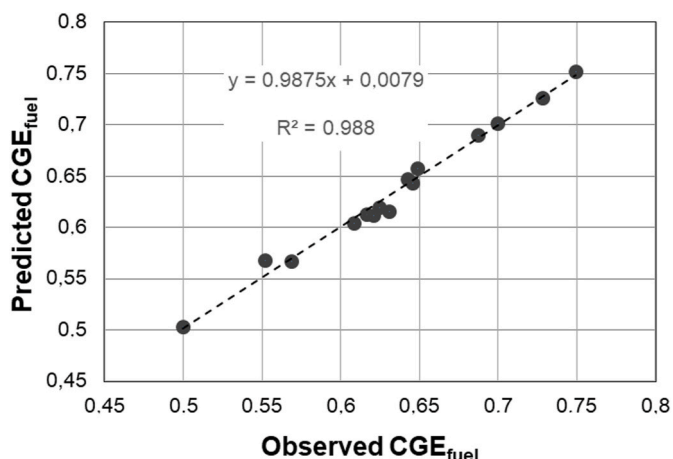


Fig. 7. Observed and model predicted CGE_{fuel} values.

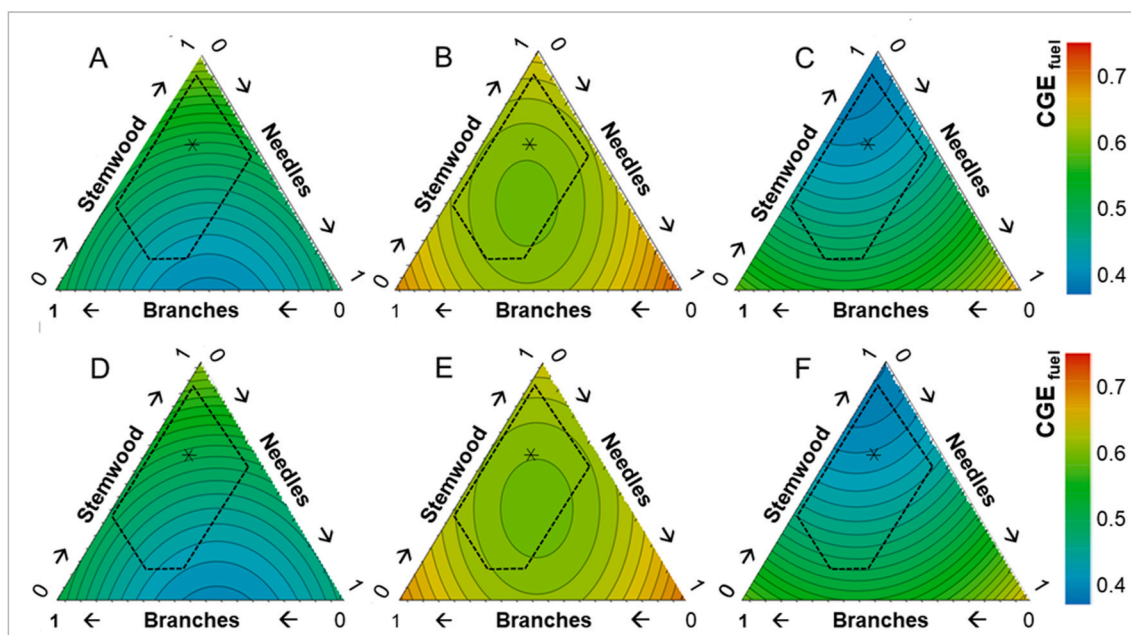


Fig. 8. Contour plot with CGE_{fuel} values according to color bar for A and D at 0.5, for B and E at 0.65 and for C and F at 0.8 kg oxygen supply per kg biomass d.a.f. when varying stemwood, branches and needles from 0 to 1 (0–100%) in the feedstock (bark set to 3.7% for A–C and to 7.6% for D–F; marked area is min and max; star is average for components in single trees).

optimal oxygen supply value for one of these components only reduced the efficiency for the other by 0.8–1.1 percentage points, although the PLS model suggested losses of 1.9–3.4 percentage points under the same conditions. For logging residues including tops, which consist of needles and branches (average contents: 32.1% and 67.9%, respectively), the predicted losses in CGE_{fuel} relative to separate gasification of the two components were up to 1.0 percentage points. Optimizing the gasification conditions for one of these components reduced the cold gas efficiency for the other by 1.6–2.2 percentage points. These losses are larger than those for stems because the difference between the optimal oxygen supply levels for branches and needles is greater than that for wood and bark. Under the same conditions, the PLS model predicted efficiency losses of 0.7–9.6 percentage points.

A few experimental studies have examined the use of biomass blends in gasification (Gomez et al., 2021; Mallick et al., 2020; Zhu et al., 2016; Sulaiman et al., 2018; Inayat et al., 2019) and a larger number have investigated co-gasification of biomass and coal (Brown et al., 2000; Collot et al., 1999; Thattai et al., 2016), coal with biomass and waste plastics (Pinto et al., 2003), or biomass and municipal solid waste (Cai et al., 2021; Pio et al., 2020). It would of course be possible to determine optimal oxygen supply levels for perfect mixtures of these feedstock blends. However, in reality the use of fuel blends tends to introduce considerable variation in feedstock composition due to imperfect mixing. For example, Gomez et al. (2021) found that CGE declined as the content of rice husks in the fuel mixture increased. This was attributed to a substantial increase in the variability of the feedstock's composition, which affected the equivalence ratio and thus caused gasification to be performed under non-optimal conditions. Similarly, Pio et al. (2020) reported high temperature fluctuations during co-gasification of biomass and refuse-derived fuel (RDF) due to the heterogeneity of the RDF.

Given these findings, it seems important to ask whether co-gasification may cause unintended or unrecognized losses in CGE_{fuel} . Although the efficiency losses predicted by the models presented here are generally modest, they do exist, so it is necessary to consider whether such losses are sustainable in the long term. The results obtained suggest that if the feedstock flow entering a gasification plant includes separated tree components, it would be best to gasify these components separately

rather than mixing them and performing co-gasification, especially for components whose optimum oxygen supply levels differ markedly.

If the composition of the feedstock entering a plant varies, it could be monitored so that the oxygen supply to the gasifier could be adjusted to maximize CGE_{fuel} . Because gasification is a fast process, this would require continuous measurement of the fuel composition with a high time resolution and fast process control of the oxygen supply so that changes in composition could be identified and accommodated using feed-forward strategies. This could be done by using fast spectroscopic sensors for on-line measurement and real-time prediction of feedstock composition, possibly based on artificial intelligence (AI) modelling. In addition to continuous monitoring of feedstock composition, spectrometers operating in the NIR (Lestander et al., 2012a; Lestander and Rhen, 2005) and X-ray (Thyrel et al., 2013) wavelength ranges can be used to measure the feedstock's moisture and ash content so as to determine its dry and ash-free biomass.

To summarize, the components obtained from Norway spruce (i.e., wood, bark, branches, needles and their mixtures) were used as representative diverse gasification feedstocks and it was experimentally demonstrated that each component generated different syngas compositions. The contents of NH_3 and HCN in the syngas were significantly higher for needles than for other components, presumably due to the needles' high N content. Furthermore, the O_2 supply per kg of dry and ash-free (d.a.f.) biomass required to maximize the syngas yield and process efficiency (CGE_{fuel}) depended on the type of fuel being gasified. Co-gasification of tree components such as stems or logging residues may lead to a lower gas quality than gasification of individual tree components.

The strategy for optimizing CGE_{fuel} in a high-temperature gasifier by separating feedstock into pure component streams (demonstrated here using spruce as a biomass model) is probably also applicable to other feedstocks with variable compositions such as wastes. Feedstock components could be mixed upstream of the gasifier if they have similar optimal oxygen to fuel ratios with respect to CGE_{fuel} but co-gasification will probably cause losses of efficiency if this criterion is ignored. This contradicts the common assumption that synergistic effects from mixing fuel streams lead to efficient co-gasification (e.g. Brown et al., 2000; Cai et al., 2021; Mallick et al., 2020). The efficiency losses due to

co-gasification may be more severe in practice than the results presented here suggest because consistent perfect fuel mixtures are probably extremely rare in real industrial practice. It should however be noted that consistent ash chemistry is important to facilitate ash handling and discharge from the gasifier. Fuel blending can help in this respect but possibly at the cost of overall gasification efficiency.

4. Conclusions

The results obtained show that if the feedstock entering a gasifier consists of diverse separated components, they should not be mixed because co-gasification may reduce cold gas efficiency if the energetic gas species CO and H₂ are used in downstream synthesis process to produce substances like jet fuels and electro fuels. This contradicts the common belief that fuel mixtures facilitate efficient co-gasification. Instead of simultaneous co-gasification it may be more resource-efficient to gasify the purest possible feedstocks separately, i.e., to perform co-gasification over time. Further research on large-scale gasification of biomass blends is needed to test this hypothesis.

CRedit authorship contribution statement

Torbjörn A. Lestander: Conceptualization, Methodology, Validation, Formal analysis, Writing – original draft, Writing – review & editing, Visualization, Project administration, Funding acquisition. **Fredrik Weiland:** Methodology, Validation, Investigation, Formal analysis, Writing – original draft, Writing – review & editing, Visualization. **Alejandro Grimm:** Writing – review & editing. **Magnus Rudolfsen:** Investigation, Writing – review & editing, Visualization. **Henrik Wiinikka:** Writing – original draft, Writing – review & editing, Visualization, Funding acquisition.

Declaration of competing interest

The authors declare that they have no known competing financial interests or personal relationships that could have appeared to influence the work reported in this paper.

Acknowledgements

We thank the Bio4Energy strategic research environment appointed by the Swedish government (www.bio4energy.se) for financial support. Gunnar Kalén and Markus Segerström are acknowledged for assistance in the preparation and pelleting of tree components. RISE ETC engineers and technicians are acknowledged for operating the gasification pilot plant.

Appendix A. Supplementary data

Supplementary data to this article can be found online at <https://doi.org/10.1016/j.jclepro.2022.133330>.

References

- Bale, C.W., Bélsisle, E., Chartrand, P., Decterov, S.A., Eriksson, G., Hack, K., Jung, I.H., Kang, Y.B., Melançon, J., Pelton, A.D., Robelin, C., Petersen, S., 2009. FactSage thermochemical software and databases - recent developments. *Calphad Comput. Coupling Phase Diagrams Thermochem.* 33 (2), 295–311.
- Bale, C.W., Bélsisle, E., Chartrand, P., Decterov, S.A., Eriksson, G., Gheribi, A.E., Hack, K., Jung, I.H., Kang, Y.B., Melançon, J., Pelton, A.D., Petersen, S., Robelin, C., Sangster, J., Spencer, P., Van Ende, M.-A., 2016. FactSage thermochemical software and databases - 2010 – 2016. *Calphad* 54, 35–53.
- Brown, R.C., Liu, Q., Norton, G., 2000. Catalytic effects observed during the co-gasification of coal and switchgrass. *Biomass Bioenergy* 18 (6), 499–506.
- Cai, J., Zeng, R., Zheng, W., Wang, S., Han, J., Li, K., Luo, M., Tang, X., 2021. Synergistic effects of co-gasification of municipal solid waste and biomass in fixed-bed gasifier. *Process Saf. Environ. Protect.* 148, 1–12.
- Carlborg, M., Weiland, F., Ma, C., Backman, R., Landälv, I., Wiinikka, H., 2018. Exposure of refractory materials during high-temperature gasification of a woody biomass and peat mixture. *J. Eur. Ceram. Soc.* 777–787.
- Carlsson, P., Wiinikka, H., Marklund, M., Gronberg, C., Pettersson, E., Lidman, M., Gebart, R., 2010. Experimental investigation of an industrial scale black liquor gasifier. 1. The effect of reactor operation parameters on product gas composition. *Fuel* 89 (12), 4025–4034.
- Collot, A.G., Zhuo, Y., Dugwell, D.R., Kandiyoti, R., 1999. Co-pyrolysis and co-gasification of coal and biomass in bench-scale fixed-bed and fluidised bed reactors. *Fuel* 78 (6), 667–679.
- Dry, M.E., 2002. The Fischer-Tropsch process: 1950-2000. *Catal. Today* 71 (3–4), 227–241.
- Dufor, A., Valin, S., Castelli, P., Thiery, S., Boissonnet, G., Zoulalian, A., Glaude, P.-A., 2009. Mechanisms and kinetics of methane thermal conversion in a syngas. *Ind. Eng. Chem. Res.* 6564–6572.
- Dupont, C., Boissonnet, G., Seiler, J.-M., Gauthier, P., Schwich, D., 2007. Study about the kinetic processes of biomass steam gasification. *Fuel* 86 (1–2), 32–40.
- Emami Taba, L., Irfan, M.F., Wan Daud, W.A.M., Chakrabarti, M.H., 2012. The effect of temperature on various parameters in coal, biomass and CO-gasification: a review. *Renew. Sustain. Energy Rev.* 16 (8), 5584–5596.
- Filipsson, J., Nordén, B., 2001. Avbarrning av skogsbränsle – Pilotstudie av aktiv avbarrning av trädrester med skotargrip vid lastning. Skogforsk Rapport No. 488. Skogforsk.
- Gilbe, C., Ohman, M., Lindstrom, E., Boström, D., Backman, R., Samuelsson, R., Burvall, J., 2008. Slagging characteristics during residential combustion of biomass pellets. *Energy Fuel* 22 (5), 3536–3543.
- Gomez, R.D., Palacio, M., Arango, J.F., Avila, A.E., Mendoza, J.M., 2021. Evaluation of the energy generation potential by an experimental characterization of residual biomass blends from Cordoba, Colombia in a downdraft gasifier. *Waste Manage. (Tucson, Ariz.)* 120, 522–529.
- Habibollahzade, A., Ahmadi, P., Rosen, M.A., 2021. Biomass gasification using various gasification agents: optimum feedstock selection, detail numerical analysis and tri-objective grey wolf optimization. *J. Clean. Prod.* 284, 124718.
- Higman, C., van der Burgt, M., 2008. Gasification. Gulf Professional Publishing, Burlington/Oxford.
- Inayat, M., Sulaiman, S.A., Kurnia, J.C., 2019. Catalytic co-gasification of coconut shells and oil palm fronds blends in the presence of cement, dolomite, and limestone: parametric optimization via Box Behnken Design. *J. Energy Inst.* 92, 871–882.
- Jand, N., Brandani, V., Foscolo, P., 2009. Thermodynamic limits and actual product yields and compositions in biomass gasification processes. *Ind. Eng. Chem. Res.* 48 (14), 6564–6572.
- Jolliffe, I.T., 1986. Principal component analysis and factor analysis. In: Jolliffe, I.T. (Ed.), *Principal Component Analysis*. Springer New York, New York, NY, pp. 115–128.
- Lange, J.-P., 2001. Methanol synthesis: a short review of technology improvements. *Catal. Today* 3–8.
- Lestander, T.A., Geladi, P., Larsson, S.H., Thyrel, M., 2012a. Near infrared image analysis for online identification and separation of wood chips with elevated levels of extractives. *J. Near Infrared Spectrosc.* 20 (5), 591–599.
- Lestander, T.A., Lundström, A., Finell, M., 2012b. Assessment of biomass functions for calculating bark proportions and ash contents of refined biomass fuels derived from major boreal tree species. *Can. J. For. Res.-Rev. Can. Rech. For.* 42 (1), 59–66.
- Lestander, T.A., Rhen, C., 2005. Multivariate NIR spectroscopy models for moisture, ash and calorific content in biofuels using bi-orthogonal partial least squares regression. *Analyst* 130 (8), 1182–1189.
- Mallick, D., Mahanta, P., Moholkar, V.S., 2020. Co-gasification of biomass blends: performance evaluation in circulating fluidized bed gasifier. *Energy* 192.
- Marklund, L.G., 1988. Biomassfunktioner för tall, gran och björk i Sverige [Biomass Functions for Pine, Spruce and Birch in Sweden], vol. 45. Department of Forest Survey, Rep.
- Nilsson, B., Nilsson, D., Thornqvist, T., 2015. Distributions and losses of logging residues at clear-felled areas during extraction for bioenergy: comparing dried- and fresh-stacked method. *Forests* 6 (11), 4212–4227.
- Oasmaa, A., Fonts, I., Pelaez-Samaniego, M.R., Garcia-Perez, M.E., Garcia-Perez, M., 2016. Pyrolysis oil multiphase behavior and phase stability: a review. *Energy Fuel* 30 (8), 6179–6200.
- Oginni, O., Singh, K., 2021. Effect of carbonization temperature on fuel and caffeine adsorption characteristics of white pine and Norway spruce needle derived biochars. *Ind. Crop. Prod.* 162.
- Ögren, Y., Gullberg, M., Wennebro, J., Sepman, A., Toth, P., Wiinikka, H., 2018. Influence of oxidizer injection angle on the entrained flow gasification of torrefied wood powder. *Fuel Process. Technol.* 181, 8–17.
- Pettersson, H., Stahl, G., 2006. Functions for below-ground biomass of *Pinus sylvestris*, *Picea abies*, *Betula pendula* and *Betula pubescens* in Sweden. *Scand. J. For. Res.* 21, 84–93.
- Pinto, F., Franco, C., André, R.N., Tavares, C., Dias, M., Gulyurtlu, I., Cabrita, I., 2003. Effect of experimental conditions on co-gasification of coal, biomass and plastics wastes with air/steam mixtures in a fluidized bed system. *Fuel* 82 (15–17), 1967–1976.
- Pio, D.T., Tarelho, L.A.C., Tavares, A.M.A., Matos, M.A.A., Silva, V., 2020. Co-gasification of refused derived fuel and biomass in a pilot-scale bubbling fluidized bed reactor. *Energy Convers. Manag.* 206, 112476.
- Qin, K., Jensen, P.A., Lin, W.G., Jensen, A.D., 2012a. Biomass gasification behavior in an entrained flow reactor: gas product distribution and soot formation. *Energy Fuel* 26 (9), 5992–6002.

- Qin, K., Lin, W., Jensen, P.A., Jensen, A.D., 2012b. High-temperature entrained flow gasification of biomass. *Fuel* 93, 589–600.
- Raisanen, T., Athanassiadis, D., 2013. Basic Chemical Composition of the Biomass Components of Pine, Spruce and Birch.
- Repola, J., 2008. Biomass equations for birch in Finland. *Silva Fenn.* 42 (4), 605–624.
- Repola, J., 2009. Biomass equations for Scots pine and Norway spruce in Finland. *Silva Fenn.* 43 (4), 625–647.
- Routa, J., Brännström, H., Anttila, P., Mäkinen, M., Jänis, J., Asikainen, A., 2017. Wood Extractives of Finnish Pine, Spruce and Birch – Availability and Optimal Sources of Compounds : A Literature Review. *Natural Resources and Bioeconomy Studies 73/2017*. Natural Resources Institute Finland, Helsinki, p. 55.
- Sikarwar, V.S., Zhao, M., Clough, P., Yao, J., Zhong, X., Memon, M.Z., Shah, N., Anthony, E.J., Fennell, P.S., 2016. An overview of advances in biomass gasification. *Energy Environ. Sci.* 9 (10), 2939–2977.
- Sulaiman, S.A., Roslan, R., Inayat, M., Naz, M.Y., 2018. Effect of blending ratio and catalyst loading on co-gasification of wood chips and coconut waste. *J. Energy Inst.* 91, 779–785.
- Surup, G.R., Hunt, A.J., Attard, T., Budarin, V.L., Forsberg, F., Arshadi, M., Abdelsayed, V., Shekhawat, D., Trubetskaya, A., 2020. The effect of wood composition and supercritical CO₂ extraction on charcoal production in ferroalloy industries. *Energy* 193, 154–167.
- Tao, G., Lestander, T.A., Geladi, P., Xiong, S., 2012. Biomass properties in association with plant species and assortments I: a synthesis based on literature data of energy properties. *Renew. Sustain. Energy Rev.* 16 (5), 3481–3506.
- Thattai, A.T., Oldenbroek, V., Schoenmakers, L., Woudstra, T., Aravind, P.V., 2016. Experimental model validation and thermodynamic assessment on high percentage (up to 70%) biomass co-gasification at the 253 MWe integrated gasification combined cycle power plant in Buggenum, The Netherlands. *Appl. Energy* 168, 381–393.
- Thyrel, M., Samuelsson, R., Finell, M., Lestander, T.A., 2013. Critical ash elements in biorefinery feedstock determined by X-ray spectroscopy. *Appl. Energy* 102, 1288–1294.
- Trubetskaya, A., Hunt, A.J., Budarin, V.L., Attard, T.M., Kling, J., Surup, G.R., Arshadi, M., Umeki, K., 2021. Supercritical extraction and microwave activation of wood wastes for enhanced syngas production and generation of fullerene-like soot particles. *Fuel Process. Technol.* 212.
- U'Ren, J.M., Lutzoni, F., Miadlikowska, J., Zimmerman, N.B., Carbone, I., May, G., Arnold, A.E., 2019. Host availability drives distributions of fungal endophytes in the imperilled boreal realm. *Nat. Ecol. Evol.* 3 (10), 1430–1437.
- Wang, L., Dibdiakova, J., 2014. Characterization of Ashes from Different Wood Parts of Norway Spruce Tree. In: Ranzi, E., KohseHoinghaus, K. (Eds.), *Iconbm: International Conference on Biomass, Pts 1 and 2*. Pp. 37–+.W.
- Weiland, F., Hedman, H., Marklund, M., Wiinikka, H., Öhrman, O., Gebart, R., 2013. Pressurized oxygen blown entrained-flow gasification of wood powder. *Energy Fuel* 27 (2), 932–941.
- Weiland, F., Lundström, S., Ögren, Y., 2021. Oxygen-blown gasification of pulp mill bark residues for synthetic fuel production. *Processes* 9 (1), 19.
- Weiland, F., Nordwaeger, M., Olofsson, I., Nordin, A., Wiinikka, H., 2014. Entrained flow gasification of torrefied wood residues. *Fuel Process. Technol.* 51–58.
- Weiland, F., Sweeney, D.J., Wiinikka, H., 2016. Extractive sampling of gas and particulates from the reactor core of an entrained flow biomass gasifier. *Energy Fuel* 30 (8), 6405–6412.
- Weiland, F., Wiinikka, H., Hedman, H., Wennebro, J., Pettersson, E., Gebart, R., 2015. Influence of process parameters on the performance of an oxygen blown entrained flow biomass gasifier. *Fuel* 153, 510–519.
- Werkelin, J., Lindberg, D., Bostrom, D., Skrifvars, B.J., Hupa, M., 2011. Ash-forming elements in four Scandinavian wood species part 3: combustion of five spruce samples. *Biomass Bioenergy* 35 (1), 725–733.
- Werkelin, J., Skrifvars, B.J., Hupa, M., 2005. Ash-forming elements in four Scandinavian wood species. Part 1: summer harvest. *Biomass Bioenergy* 29 (6), 451–466.
- Werkelin, J., Skrifvars, B.J., Zevenhoven, M., Holmbom, B., Hupa, M., 2010. Chemical forms of ash-forming elements in woody biomass fuels. *Fuel* 89 (2), 481–493.
- Wiinikka, H., Hage, F.S., Ramasse, Q.M., Toth, P., 2021. Spatial distribution of metallic heteroatoms in soot nanostructure mapped by aberration-corrected STEM-EELS. *Carbon* 173, 953–967.
- Wiinikka, H., Johansson, A.C., Wennebro, J., Carlsson, P., Öhrman, O.G.W., 2015. Evaluation of black liquor gasification intended for synthetic fuel or power production. *Fuel Process. Technol.* 139, 216–225.
- Wiinikka, H., Toth, P., Jansson, K., Molinder, R., Brostrom, M., Sandstrom, L., Lighty, J. S., Weiland, F., 2018. Particle formation during pressurized entrained flow gasification of wood powder: effects of process conditions on chemical composition, nanostructure, and reactivity. *Combust. Flame* 189, 240–256.
- Wiinikka, H., Weiland, F., Pettersson, E., Öhrman, O., Carlsson, P., Stjernberg, J., 2014. Characterisation of submicron particles produced during oxygen blown entrained flow gasification of biomass. *Combust. Flame* 161 (7), 1923–1934.
- Wiinikka, H., Wennebro, J., Gullberg, M., Pettersson, E., Weiland, F., 2017. Pure oxygen fixed-bed gasification of wood under high temperature (> 1000 degrees C) freeboard conditions. *Appl. Energy* 191, 153–162.
- Wold, S., Martens, H., Wold, H.O.A., 1983. The multivariate calibration problem in chemistry solved by the PLS method. In: Kågström, B., Ruhe, A. (Eds.), *Matrix Pencils*. Springer Berlin Heidelberg, pp. 286–293.
- Zhu, Y., Piotrowska, P., van Eyk, P.J., Boström, D., Wu, X., Boman, C., Broström, M., Zhang, J., Kwong, C.W., Wang, D., Cole, A.J., de Nys, R., Gentili, F.G., Ashman, P.J., 2016. Fluidized bed co-gasification of algae and wood pellets: gas yields and bed agglomeration analysis. *Energy Fuel* 30, 1800–1809.